UCLA
COMPUTATIONAL AND APPLIED MATHEMATICS

Fourier Analysis of Incomplete Factorization Preconditioners for 3D Anisotropic Problems

June M. Donato
Tony F. Chan

December 1990

CAM Report 90-31

Department of Mathematics
University of California, Los Angeles
Los Angeles, CA. 90024-1555

FOURIER ANALYSIS OF INCOMPLETE FACTORIZATION PRECONDITIONERS FOR 3D ANISOTROPIC PROBLEMS*

JUNE M. DONATO† AND TONY F. CHAN‡

Abstract. To solve three-dimensional elliptic problems using preconditioned conjugate gradient it is crucial to make a good choice of preconditioner. To facilitate this choice a Fourier analysis technique has been used by Chan and Elman [7] and by Chan and Meurant [8] to study preconditioned systems arising from the discretization of the 2D model elliptic equation. In this paper we use the same technique to analyze relaxed-modified incomplete factorization preconditioned systems that arise from the discretization of a 3D anisotropic elliptic problem. Expressions for the 'Fourier eigenvalues' of the preconditioned 3D systems are presented along with estimates of the condition numbers. For MILU, an optimal value for the parameter c is derived. The correlation between the distribution of the eigenvalues and the Fourier results for the preconditioned systems is remarkable. From the expressions for the eigenvalues we prove that $\kappa(M^{-1}A)$ is order h^{-2} for ILU and order h^{-1} for MILU($c \neq 0$). Then by examining the distribution of Fourier eigenvalues we can exemplify the dependence of PCG convergence rate on the clustering of the eigenvalues of an operator as well as its condition number. The PCG experiments were performed on an Alliant FX/80.

Key Words. Fourier analysis, three-dimensional problems, periodic and Dirichlet boundary conditions, condition numbers.

AMS(MOS) subject classification. 65F10, 65N20; secondary 15A06

1. Introduction. While preconditioned conjugate gradient (PCG) is a widely used method of solving systems arising from the discretization of elliptic partial differential equations (PDEs), its performance is highly dependent upon the preconditioner chosen. For 2D discretized elliptic PDEs much theory and experimental background exists for the use of ILU and MILU preconditioned systems [3, 4, 6, 12, 13]. However for 3D problems there is considerably less knowledge [1, 2, 14, 15]. Experimental difficulties arise because the discretization of 3D problems leads to extremely large systems. Even though these systems are typically sparse, the space and time requirements are still daunting on most sequential machines. Hence, we see the move to parallel computers. But still the choice of a 'good' preconditioner remains.

To facilitate this choice a Fourier analysis technique has been used by Chan and Elman [7] and by Chan and Meurant [8] to study preconditioned systems arising from the discretization of the 2D model elliptic equation. In this paper we use the same technique to analyze relaxed-modified incomplete factorization preconditioned systems that arise from the discretization of a 3D anisotropic elliptic problem.

We begin by considering the matrix A arising from the discretization of 3D anisotropic

* This work was supported in part by the Department of Energy under contract DEFG03-87-ER-25037 and the Army Research Office under contract DAAL03-88-K-0085. This version was last modified December 21, 1990.

† Also supported by NASA Grant NGT-70125. Department of Mathematics, UCLA, Los Angeles, CA 90034. E-mail: donato@math.ucla.edu

‡ Department of Mathematics, UCLA, Los Angeles, CA 90034. E-mail: chan@math.ucla.edu or na.tchan@na-net.stanford.edu.

elliptic problems. For the preconditioner M we will examine (point) relaxed-modified incomplete LU factorizations. (For experiments using point and block methods see [2, 15].) Using the Fourier technique of [7], the resulting preconditioned systems $M^{-1}A$ are analyzed. Expressions for the 'Fourier eigenvalues' are given and from these expressions we derive bounds on the condition numbers. For the isotropic problem we find, as in the 2D case [7], that $\kappa(M^{-1}A)$ is order h^{-2} for ILU and and h^{-1} for MILU ($c \neq 0$). For MILU, an optimal value of c_{opt} is derived.

To examine the usefulness of these Fourier derivations and calculations, we present the results of a PCG implementation for comparison. Because of the inherent large size of these 3D problems, the PCG algorithm was coded on an Alliant FX/80 using FX/FORTRAN. We examine various grid spacings and their effect upon condition numbers and iterations required for convergence. We find the dependence on h of the preconditioned Dirichlet and periodic operators to be in remarkable agreement. For the anisotropic problem we illustrate the dependence of PCG convergence on the distribution of eigenvalues [3, 4] and show that the clustering of the Fourier eigenvalues mimics that of the Dirichlet eigenvalues.

For many of the experiments, the distribution of the eigenvalues is given for both the preconditioned Dirichlet and the related periodic systems. While true Fourier analysis is not directly applicable to these problems, it is obvious from our numerical results that the Fourier technique is an extremely valuable heuristic method for examining the behavior of these preconditioned systems. The method is easy to apply and can save considerable time by determining initial approximations to optimal parameters. It is worth noting that the use of Fourier methods is a long standing technique for the analysis of multigrid. A notable example is Brandt's 'local mode analysis' [5].

The rest of this paper is outlined as follows. In Section 2 the stencil and recurrence relation are given for the general relaxed-(M)ILU preconditioner. In Section 3 the Fourier eigenvalues are derived for the related periodic preconditioned operator for the general anisotropic problem and theorems for the isotropic problem are stated for ILU and MILU preconditioned systems. In Section 4 we give background information on the codes used. We also present various experimental results and we compare predicted results to the actual numerical results from the PCG implementation. In Section 5 is a summary of conclusions. And finally in the Appendix are the proofs of the Fourier theorems and the derivation of c_{opt}.

2. The Preconditioner. We start by considering the following 3D anisotropic equation as our expanded model problem

$$-\left(a_1 u_{xx} + a_2 u_{yy} + a_3 u_{zz}\right) = r \tag{1}$$

posed on the unit cube $\Omega = \{0 \leq x, y, z \leq 1\}$ with $a_1, a_2, a_3 \geq 0$ and Dirichlet boundary conditions

$$u(x, y, z) = 0 \text{ on } \partial\Omega. \tag{2}$$

The problem is then discretized on the interior of the unit cube by the standard second order finite differences using a uniform $n \times n \times n$ mesh with mesh size $h = \frac{1}{n+1}$.

We get a matrix system $Au = b$ where A is represented by a 7-point stencil. The general 7-point stencil for the Dirichlet problem yields a linear equation of the form

$$\begin{aligned} a_{i,j,k}u_{i,j,k} &+ b_{i,j,k}u_{i+1,j,k} + c_{i,j,k}u_{i,j+1,k} + d_{i,j,k}u_{i-1,j,k} + e_{i,j,k}u_{i,j-1,k} \\ &+ f_{i,j,k}u_{i,j,k+1} + g_{i,j,k}u_{i,j,k-1} \\ &= h^2 r_{i,j,k} \end{aligned} \tag{3}$$

where $1 \leq i, j, k \leq n$ and

$$\begin{aligned} b_{i,j,k} &= 0, \quad i = n \\ c_{i,j,k} &= 0, \quad j = n \\ f_{i,j,k} &= 0, \quad k = n \\ d_{i,j,k} &= 0, \quad i = 1 \\ e_{i,j,k} &= 0, \quad j = 1 \\ g_{i,j,k} &= 0, \quad k = 1 \end{aligned} \tag{4}$$

Note that the subscripts (i, j, k) correspond to the grid location (ih, jh, kh). For example, the entry $b_{i,j,k}$ represents the coupling between $u_{i,j,k}$ and its neighbor $u_{i+1,j,k}$. Writing the left-hand-side in stencil form (expanding by planes) we have

$k-1$ plane			k plane			$k+1$ plane		
·	·	·	·	$c_{i,j,k}$	·	·	·	·
·	$g_{i,j,k}$	·	$d_{i,j,k}$	$a_{i,j,k}$	$b_{i,j,k}$	·	$f_{i,j,k}$	·
·	·	·	·	$e_{i,j,k}$	·	·	·	·

Referring back to the anisotropic problem we have the assignments

$$\begin{aligned} a_{i,j,k} &= 2(a_1 + a_2 + a_3) \\ b_{i,j,k} &= -a_1 \\ c_{i,j,k} &= -a_2 \\ d_{i,j,k} &= -a_1 \\ e_{i,j,k} &= -a_2 \\ f_{i,j,k} &= -a_3 \\ g_{i,j,k} &= -a_3 \end{aligned} \tag{5}$$

A relaxed-modified ILU factorization is an approximate LU factorization M of A based on Gaussian Elimination in which non-zero entries (fill-ins) of L and U are dropped (set to zero) if they correspond to a zero element in A (*i.e.* the sparsity patterns for L and U are the same as for A). Further, the non-zero entries of the resulting matrix $M = LU$ are required to equal the corresponding non-zero entries of A except possibly for those entries along the diagonal. For example, for ILU it is required that $diag(M) = diag(A)$. For MILU(c), the diagonal of M is modified to ensure the condition $rowsum(M) = rowsum(A) + ch^2$. Hence, in MILU a fill-in in a row of M is added onto the diagonal element of that row of M along with the perturbation ch^2. For RILU(w), only a fraction w of the fill-ins are added back onto the diagonal of M. In this paper, we further restrict U to be unit diagonal.

Using the stencil viewpoint, the (relaxed-modified) LU factorization of A has the following structure where L is the lower triangular matrix

$k-1$ plane			k plane			$k+1$ plane		
·	·	·	·	·	·	·	·	·
·	$g_{i,j,k}$	·	$d_{i,j,k}$	$\alpha_{i,j,k}$	·	·	·	·
·	·	·	·	$e_{i,j,k}$	·	·	·	·

and U is the unit upper triangular matrix given by

$k-1$ plane			k plane			$k+1$ plane		
·	·	·	·	$\frac{c_{i,j,k}}{\alpha_{i,j,k}}$	·	·	·	·
·	·	·	·	1	$\frac{b_{i,j,k}}{\alpha_{i,j,k}}$	·	$\frac{f_{i,j,k}}{\alpha_{i,j,k}}$	·
·	·	·	·	·	·	·	·	·

The resulting preconditioner $M = LU$ is then represented by

$k-1$ plane			k plane			$k+1$ plane		
·	$m_{i+1,j,k-1}$	·	$m_{i-1,j+1,k}$	$c_{i,j,k}$	·	·	·	·
·	$g_{i,j,k}$	$m_{i,j+1,k-1}$	$d_{i,j,k}$	$m_{i,j,k}$	$b_{i,j,k}$	$m_{i-1,j,k+1}$	$f_{i,j,k}$	·
·	·	·	·	$e_{i,j,k}$	$m_{i+1,j-1,k}$	·	$m_{i,j-1,k+1}$	·

The center (diagonal) entries $m_{i,j,k}$ of M are given by

$$m_{i,j,k} = \alpha_{i,j,k} + d_{i,j,k}\frac{b_{i-1,j,k}}{\alpha_{i-1,j,k}} + e_{i,j,k}\frac{c_{i,j-1,k}}{\alpha_{i,j-1,k}} + g_{i,j,k}\frac{f_{i,j,k-1}}{\alpha_{i,j,k-1}}.$$

The other six entries of M that correspond to zero elements in A are called the 'fill-ins.' They are given by

$$
\begin{aligned}
m_{i+1,j,k-1} &= g_{i,j,k}\frac{b_{i,j,k-1}}{\alpha_{i,j,k-1}} \\
m_{i,j+1,k-1} &= g_{i,j,k}\frac{c_{i,j,k-1}}{\alpha_{i,j,k-1}} \\
m_{i-1,j+1,k} &= d_{i,j,k}\frac{c_{i-1,j,k}}{\alpha_{i-1,j,k}} \\
m_{i+1,j-1,k} &= e_{i,j,k}\frac{b_{i,j-1,k}}{\alpha_{i,j-1,k}} \\
m_{i-1,j,k+1} &= d_{i,j,k}\frac{f_{i-1,j,k}}{\alpha_{i-1,j,k}} \\
m_{i,j-1,k+1} &= e_{i,j,k}\frac{f_{i,j-1,k}}{\alpha_{i,j-1,k}}
\end{aligned}
\tag{6}
$$

To determine the $\alpha_{i,j,k}$ values, the Relaxed Modified LU factorization is typically augmented by the rowsum condition

$$rowsum(M) = rowsum(A) + ch^2 + (1-w) * (\text{fill-ins in } M).$$

The above formulation includes both the parameter $\delta = ch^2$ of Gustafsson [12] which is added to the main diagonal and a relaxation parameter w of Axelsson and Lindskog [3]. (See also [1].) This condition yields the ILU factorization for $c = w = 0$ and MILU(c) for $w = 1$. For $c = 0, w \in (0,1)$ we get RILU(w) [6, 10].

Given that six of the entries in any given row are common to both A and M, the rowsum condition yields a second expression for the diagonal entries of M

$$m_{i,j,k} = a_{i,j,k} + ch^2 - w(\text{fill-ins in } M).$$

Substituting in the expressions for the fill-ins and for $m_{i,j,k}$ the following recurrence for $\alpha_{i,j,k}$ results

$$
\begin{aligned}
\alpha_{i,j,k} = a_{i,j,k} + ch^2 &- d_{i,j,k}(b_{i-1,j,k} + w(c_{i-1,j,k} + f_{i-1,j,k}))/\alpha_{i-1,j,k} \\
&- e_{i,j,k}(c_{i,j-1,k} + w(b_{i,j-1,k} + f_{i,j-1,k}))/\alpha_{i,j-1,k} \\
&- g_{i,j,k}(f_{i,j,k-1} + w(b_{i,j,k-1} + c_{i,j,k-1}))/\alpha_{i,j,k-1}
\end{aligned}
\tag{7}
$$

where (4) applies and a term is ignored if it involves an $\alpha_{i,j,k}$ having any of its indices equal to 0 or $n+1$.

3. Fourier Analysis. A method of exact analysis of $M^{-1}A$ has not yet presented itself. Yet it is critical to be able to compare the distribution of the resulting eigenvalues and their clustering traits for different preconditioners M. These clustering traits along with the condition number, $\kappa(M^{-1}A)$, affect the convergence rate of a PCG method [3, 4]. So our basic approach here, while not exact, is to find the Fourier transform of $M^{-1}A$. We do this by applying $M^{-1}A$ to the eigenvectors $u^{(s,t,r)}$ composed of Fourier exponential modes. The $(i,j,k)^{th}$ grid component of $u^{(s,t,r)}$ is given by

$$u_{ijk}^{(s,t,r)} = e^{\iota i\theta_s} e^{\iota j\phi_t} e^{\iota k\xi_r}$$

where $\iota = \sqrt{-1}$, $\theta_s = \frac{2\pi}{n+1}s$, $\phi_t = \frac{2\pi}{n+1}t$, $\xi_r = \frac{2\pi}{n+1}r$, for $r, s, t = 1, ..., n$.

However, this technique is theoretically exact only for constant coefficient problems with periodic boundary conditions [7]. In other words, the $u^{(s,t,r)}$ are not eigenvectors of the matrix $M^{-1}A$ that results from the discretization of the Dirichlet problem. To use the technique we make the following extensions [7]:

(a) Treat the matrices M and A as if they were periodic. Enforce equations (5) for $0 \le i, j, k \le n+1$ and ignore the Dirichlet constraints (4).

(b) Force M to be a constant diagonal system by treating the $\alpha_{i,j,k}$ as the constant α arising as the asymptotic solution of the recurrence equation (7). So $\alpha_{i,j,k} = \alpha$ is then given by

$$\begin{aligned} \alpha \;=\; & \left((a_1+a_2+a_3)+\frac{ch^2}{2}\right) \\ (8) \qquad + & \sqrt{\left((a_1+a_2+a_3)+\frac{ch^2}{2}\right)^2 - (a_1^2+a_2^2+a_3^2) - 2w(a_1a_2+a_1a_3+a_2a_3)} \end{aligned}$$

where the positive root has been chosen to agree in magnitude with the Dirichlet values. In the case of very large n, this is the value the $\alpha_{i,j,k}$ would tend toward for those (i,j,k) corresponding to grid points far from the boundaries of Ω. The proof that $\alpha_{i,i,i} \searrow \alpha$ follows analogously to the 2D situation given in [16].

(c) From the theory developed in [7], we then use the formula $h_d = 2h_p$ to relate the mesh sizes used for the Dirichlet problem to that of the corresponding Fourier method (periodic) result.

With the above extensions, we have obtained a periodic constant coefficient ILU factorization preconditioner for which exact Fourier analysis can be used. Note that this related periodic ILU factorization is not the ILU factorization for the periodic version of the Dirichlet problem. It is an artificial operator which we analyze in the hope that the results will apply to the ILU preconditioned Dirichlet system.

Now applying these related periodic extensions of A and M to $u^{(s,t,r)}$ yields

$$\begin{aligned} Au^{(s,t,r)} &= \lambda_{str} u^{(s,t,r)} \\ Mu^{(s,t,r)} &= \psi_{str} u^{(s,t,r)} \end{aligned}$$

where

$$\lambda_{str} = \lambda_{str}(A) = 4(a_1 \sin^2(\frac{\theta_s}{2}) + a_2 \sin^2(\frac{\phi_t}{2}) + a_3 \sin^2(\frac{\xi_r}{2})) \tag{9}$$

and

$$\begin{aligned} \psi_{str} &= \psi_{str}(M) \\ &= \lambda_{str} + \frac{2}{\alpha}(a_1 a_2 \cos(\theta_s - \phi_t) + a_1 a_3 \cos(\xi_r - \theta_s) + a_2 a_3 \cos(\phi_t - \xi_r)) \\ &\quad - 2w(a_1 a_2 + a_1 a_3 + a_2 a_3)/\alpha + ch^2. \end{aligned} \tag{10}$$

Thus, the Fourier transform of $M^{-1}A$ is

$$\mu_{str}(M^{-1}A) = \frac{\lambda_{str}(A)}{\psi_{str}(M)} \tag{11}$$

and the condition number of the preconditioned system is given by

$$\kappa = \kappa(M^{-1}A) = \frac{\max_{str} \mu_{str}}{\min_{str} \mu_{str}}.$$

From (9) and (10) this can be easily computed for a given mesh size h. The n^3 values μ_{str} are also called the Fourier eigenvalues of $M^{-1}A$.

Consider for now the isotropic problem ($a_1 = a_2 = a_3 = 1$). Using the above we get the following results whose proofs are presented in the Appendix.

THEOREM 3.1. *For the ILU preconditioned isotropic operator* ($w = 0, c = 0$),

$$\kappa^{(I)} = O(h^{-2}).$$

THEOREM 3.2. *For the MILU preconditioned isotropic operator* ($w = 1$),

$$\kappa^{(M)} = \begin{cases} O(h^{-1}), & \text{if } c > 0; \\ O(h^{-2}), & c = 0. \end{cases}$$

Result 3.1. The optimal value of c occurs near $c_p = 12\pi^2$ for the periodic problem and $c_d = 3\pi^2$ for the Dirichlet problem.

It appears from numerical calculations below that the above results also hold for the Dirichlet ILU and MILU preconditioned systems except for MILU when c is near zero. And in the anisotropic cases, although generalizing these theorems poses some difficulties, we are able to show that the Fourier results are still excellent predictors of the Dirichlet results in terms of dependence on h and c.

4. Numerical Results. In order to verify the preceding Fourier results, a PCG routine was implemented on an Alliant FX/80 to solve the system $Au = b$ using equations (3), (4) and (5) where the true solution was chosen to be

$$u(x, y, z) = x(1 - x)y(1 - y)z(1 - z).$$

Except where noted, uniformly distributed random initial data [1] was used for u on the interior of the unit cube.

In order to compare condition numbers for small h we approximated the extreme eigenvalues of the (M)ILU preconditioned systems from PCG generated values as outlined in [11]. From values generated during the PCG iterations, a symmetric tridiagonal matrix associated with the Lanczos vectors is generated. An EISPACK routine is then called to determine the eigenvalues of the tridiagonal matrix which will in turn approximate the extreme eigenvalues of the preconditioned system. All computations were done in double precision except for the EISPACK routine. The stopping criterion for the PCG iteration required the following three conditions to be satisfied concurrently

$$\frac{\|r^{(k)}\|}{\|r^{(0)}\|} < 10^{-14},\ |\mu_{min}^{(k)} - \mu_{min}^{(k-1)}| < 10^{-3} \text{ and } |\mu_{max}^{(k)} - \mu_{max}^{(k-1)}| < 10^{-3}.$$

For some experimental results the full set of eigenvalues was needed for the preconditioned operator. A full set of eigenvalues could only be generated in reasonable time for large h (small n). For this a separate program was implemented wherein the M and A matrices were generated and then a call to another EISPACK routine was made to solve the general eigenvalue problem $Ax = \mu Mx$.

A routine to generate the Fourier eigenvalues and condition numbers via equations (8), (9), and (10) was implemented on a Sun 3/150 workstation. The computations were performed in double precision.

4.1. ILU results ($c = w = 0$). First, we show that the Fourier technique predicts the distribution of the eigenvalues for the ILU preconditioned Dirichlet operator. Figure 1 shows the distribution of the eigenvalues of the preconditioned Dirichlet and periodic operators for $h_d = 1/8$ ($h_p = 1/16$). The range and clustering of the Dirichlet ILU and the Fourier ILU eigenvalues are extremely close. Table 1 shows the results for various values of h for the ILU preconditioned Dirichlet problem. As h decreases the Fourier results (Table 2) for the minimum and maximum eigenvalue (and hence condition number) are closer to those for the preconditioned Dirichlet system. As predicted, $\kappa(M^{-1}A) = O(h^{-2})$ in each case.

[1] Experiments were also performed with zero initial data and normally distributed random initial data. Qualitatively the results did not depend on the choice of these initial data.

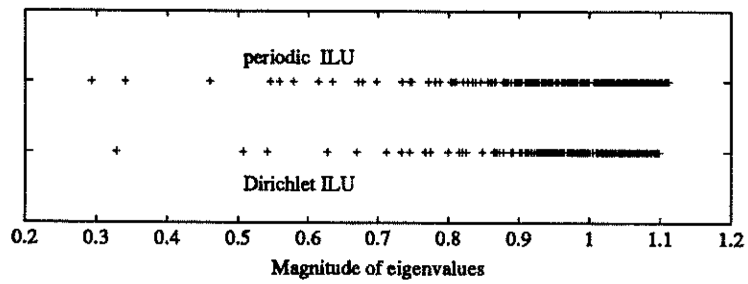

FIG. 1. *Eigenvalues of the isotropic ILU preconditioned system,* $h_d = \frac{1}{8}$ $(h_p = \frac{1}{16})$

TABLE 1
Dirichlet ILU results for various h_d *values*

h_d	$\min \mu$	$\max \mu$	$\kappa(M^{-1}A)$
1/8	0.328	1.096	3.341
1/16	0.098	1.108	11.281
1/32	0.0258	1.111	43.045
1/64	0.0065	1.112	170.123

TABLE 2
Periodic ILU results for corresponding h_p

h_d	$\min \mu$	$\max \mu$	$\kappa(M^{-1}A)$
1/8	0.293	1.112	3.791
1/16	0.095	1.112	11.735
1/32	0.026	1.112	43.503
1/64	0.0065	1.112	170.574

4.2. MILU results $w = 1$. In Figure 2 the minimum and maximum eigenvalues and the condition numbers are plotted as a function of c for $h_d = 1/8$ for the Dirichlet operator and $h_p = 1/16$ for the Periodic MILU results.

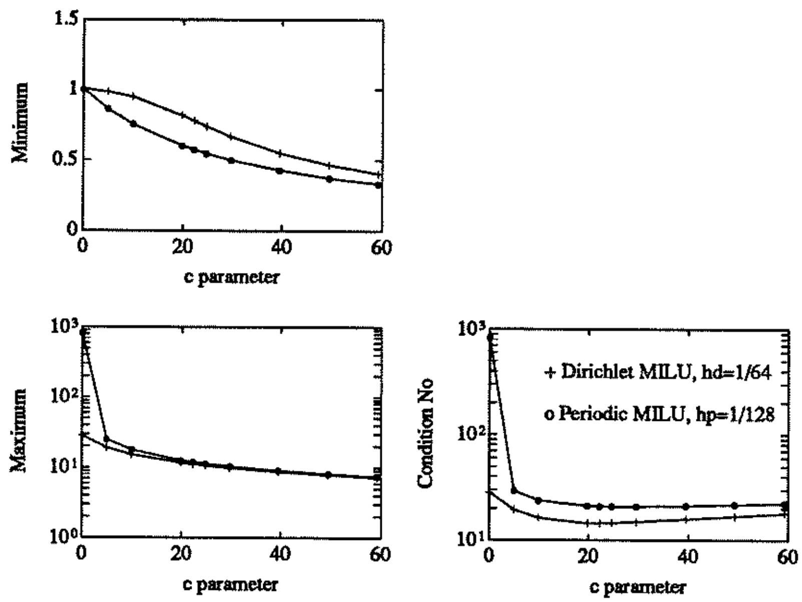

FIG. 2. *MILU results as a function of c for* $h_d = \frac{1}{64}$

For large c, the maximum eigenvalues are indistinguishable. For the minimum eigenvalues (and hence the condition numbers) the values are different, but the trend in the values as functions of increasing c are similar. Also we see from Figure 2 that the optimal c value for the MILU preconditioned Dirichlet operator does occur at c slightly less than the value $c_d = 3\pi^2$ predicted by Result 3.1.

TABLE 3
Dirichlet MILU results for $c = 3\pi^2$

h_d	$\min\mu$	$\max\mu$	$\kappa(M^{-1}A)$
1/8	0.537	1.444	2.689
1/16	0.585	2.614	4.465
1/32	0.629	5.018	7.971
1/64	0.664	9.872	14.871

TABLE 4
periodic MILU results for $c = 3\pi^2$

h_d	$\min\mu$	$\max\mu$	$\kappa(M^{-1}A)$
1/8	0.497	1.545	3.110
1/16	0.499	2.797	5.603
1/32	0.500	5.341	10.687
1/64	0.500	10.429	20.859

TABLE 5
Dirichlet MILU results for $c = 0$

h_d	$\min\mu$	$\max\mu$	$\kappa(M^{-1}A)$
1/8	1.000	2.753	2.753
1/16	1.000	5.983	5.982
1/32	1.000	13.125	13.120
1/64	1.001	28.256	28.337

TABLE 6
periodic MILU results for $c = 0$

h_d	$\min\mu$	$\max\mu$	$\kappa(M^{-1}A)$
1/8	1.000	13.252	13.252
1/16	1.000	52.156	52.156
1/32	1.000	207.784	207.784
1/64	1.000	830.301	830.301

Tables 3 and 4 contain the results for various values of h_d for $c_d = 3\pi^2$. We see that the Periodic values for MILU are not as close to the Dirichlet values as they were for the ILU case. But we do see that the Periodic results display the $O(h^{-1})$ behavior that occurs for the MILU operator for $c_d = 3\pi^2$.

Tables 5 and 6 show the corresponding results for $c = 0$. The Periodic MILU condition number displays $O(h^{-2})$ behavior rather than the $O(h^{-1})$ behavior of the Dirichlet MILU operator. This is the same situation that arises for the 2D case [7]. For $c = 0$, it takes a very delicate cancellation to yield the $O(h^{-2})$ results for the Fourier condition number. Away from $c = 0$ the calculations are not as delicate and the Fourier prediction is very good.

Figure 3 plots the condition number of the MILU preconditioned Dirichlet problem and the Fourier condition number results for $h_d = 1/16$ (the lower two curves) and for $h_d = 1/64$ (the upper two curves). Again, we see that away from $c = 0$ the dependence of conditioning on the parameter c clearly follows the same general pattern for the preconditioned Dirichlet operator (a given h_d) and its corresponding Fourier results ($h_p = h_d/2$).

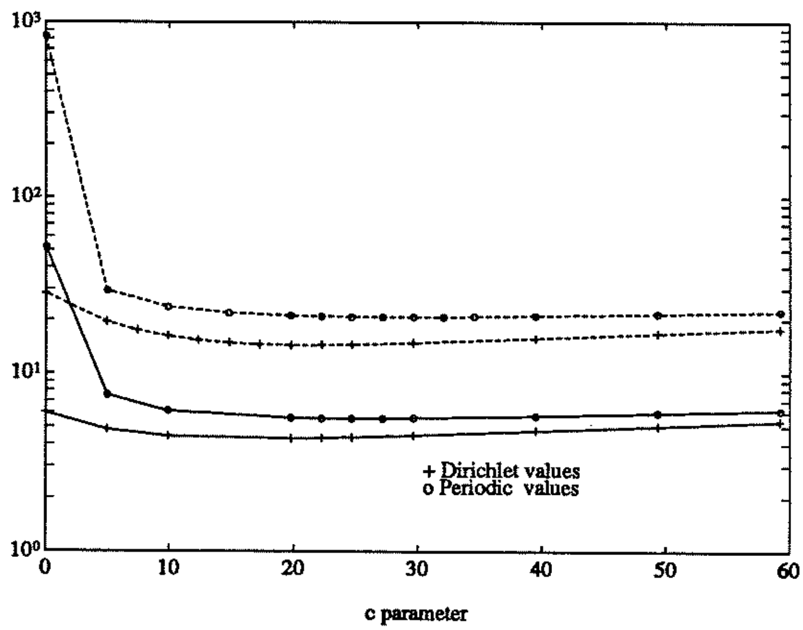

FIG. 3. *MILU condition numbers for $h_d = \frac{1}{16}$(solid lines) and $h_d = \frac{1}{64}$(dashed lines)*

4.3. Anisotropic Results. To examine results from anisotropic problems we pick the following three sets of data

Data Set 1: $a_1 = a_2 = a_3 = 1$

Data Set 2: $a_1 = 1, a_2 = 1, a_3 = 0.01$

Data Set 3: $a_1 = 1, a_2 = 0.01, a_3 = 0.01$

These three data sets are a subset of those used in [2]. And to allow us to compare results to [2] we use an initial guess for $u(x, y, z)$ that is zero on the interior of the unit cube.

Tables 7, 8 and 9 present the results for $h = 1/21$ for the ILU preconditioned operators. For each of the three data sets the periodic ILU results are in close approximation of the Dirichlet ILU values. In particular, the behavior of the Dirichlet ILU condition numbers is captured by the periodic ILU condition numbers. What is of further interest is the comparison of condition numbers and PCG iteration counts for the Dirichlet ILU operator across the three data sets. $\kappa(M^{-1}A)$ for data set 1 is greater than κ for data set 2. Yet data set 1 requires significantly fewer PCG iterations to converge than data set 2. This iteration count variation is also seen in the data presented in [2].

TABLE 7
ILU results for Data Set 1

$h_d = 1/21$	$\min \mu$	$\max \mu$	$\kappa(M^{-1}A)$	iterations
ILU	0.059	1.108	18.900	37
periodic	0.057	1.112	19.388	na

TABLE 8
ILU results for Data Set 2

$h_d = 1/21$	$\min \mu$	$\max \mu$	$\kappa(M^{-1}A)$	iterations
ILU	0.072	1.198	16.667	57
periodic	0.070	1.203	17.106	na

TABLE 9
ILU results for Data Set 3

$h_d = 1/21$	$\min \mu$	$\max \mu$	$\kappa(M^{-1}A)$	iterations
ILU	0.419	1.436	3.426	27
periodic	0.479	1.472	3.600	na

To study this more closely we redo the calculations for $h_d = 1/8$ so that the full set of eigenvalues can be plotted. Tables 10, 11 and 12 present the minimum, maximum and condition number results for the three data sets and we see that the same situation occurs as for $h_d = 1/21$. In Figure 4, the eigenvalues of the Dirichlet ILU operator are plotted in sorted order for data sets 2 and 3 with $h_d = 1/8$. These figures also include the Fourier eigenvalues for $h_p = 1/16$.

For the corresponding figure for data set 1, refer back to figure 1.

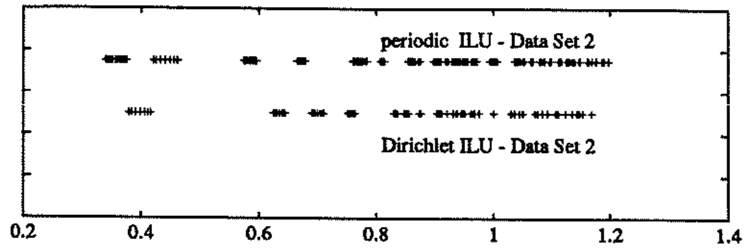

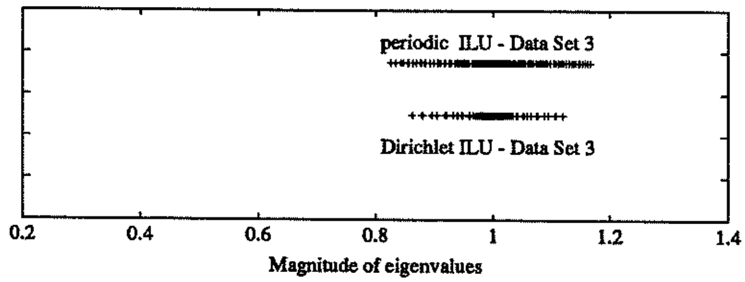

FIG. 4. *Eigenvalues for the anisotropic ILU preconditioned systems,* $h_d = \frac{1}{8}$ $(h_p = \frac{1}{16})$

First we notice the extreme similarity of the Dirichlet and Fourier eigenvalues. For each data set the behavior of the Fourier eigenvalues corresponds to that of the preconditioned Dirichlet system. And we can see using either the Dirichlet or Fourier spectra that it is the clustering [3, 4] of the eigenvalues that becomes the dominant factor in the number of iterations required.

Data set 1 yields a larger condition number than data set 2 because (in part) of its much smaller minimum eigenvalue. But data set 1 has only a few well isolated minimum eigenvalues whereas there is a clustering of eigenvalues near the minimum for data set 2. The eigenvalues for data set 1 have more clustering about 1 than those for data set 2. Hence, the systems from data set 1 converge more quickly via PCG than those from data set 2.

For data set 2, table 13 lists the condition number of the ILU preconditioned system as a function of h. Table 14 similarly reports the results for data set 3.

We see the remarkable agreement of the ILU and Fourier results that occurred in the isotropic case for ILU. Hence, the Fourier results remain a good predictor of the dependence of $\kappa(M^{-1}A)$ on h.

TABLE 10

ILU results for Data Set 1

$h_d = 1/8$	$\min \mu$	$\max \mu$	$\kappa(M^{-1}A)$	iterations
ILU	0.328	1.095	3.338	16
periodic	0.293	1.112	3.791	na

TABLE 11

ILU results for Data Set 2

$h_d = 1/8$	$\min \mu$	$\max \mu$	$\kappa(M^{-1}A)$	iterations
ILU	0.379	1.168	3.079	20
periodic	0.340	1.199	3.523	na

TABLE 12

ILU results for Data Set 3

$h_d = 1/8$	$\min \mu$	$\max \mu$	$\kappa(M^{-1}A)$	iterations
ILU	0.863	1.119	1.297	14
periodic	0.825	1.166	1.413	na

TABLE 13

Data Set 2: $\kappa(M^{-1}A)$ for various h

h_d	ILU	Periodic
1/8	3.079	3.523
1/16	10.002	10.446
1/32	37.667	38.096

TABLE 14

Data Set 3: $\kappa(M^{-1}A)$ for various h

h_d	ILU	Periodic
1/8	1.297	1.413
1/16	2.369	2.546
1/32	6.667	6.857

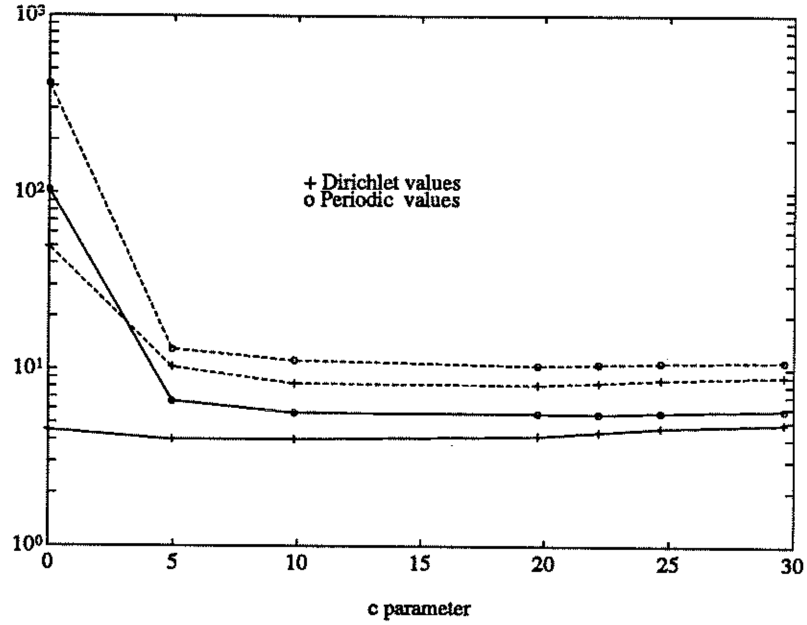

FIG. 5. $\kappa(M^{-1}A)$ *for anisotropic MILU for data set 2,* $h_d = \frac{1}{16}$*(solid lines),* $h_d = \frac{1}{32}$*(dashed lines)*

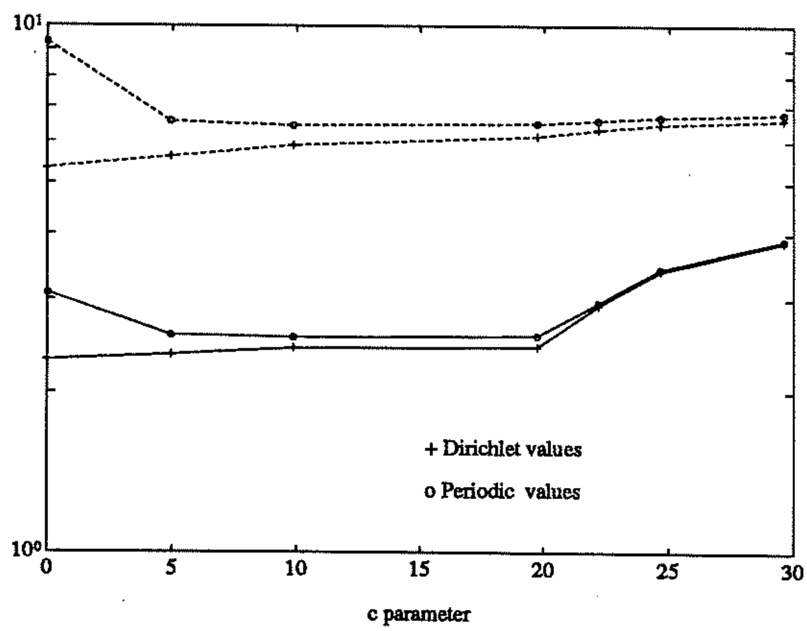

FIG. 6. $\kappa(M^{-1}A)$ *for anisotropic MILU for data set 3,* $h_d = \frac{1}{16}$*(solid lines),* $h_d = \frac{1}{32}$*(dashed lines)*

TABLE 15

$\kappa(M^{-1}A)$ results for MILU ($c_d = 2\pi^2$) preconditioned system for Data Set 1

h_d	MILU	Periodic
1/8	2.521	3.032
1/16	4.282	5.619
1/32	7.721	10.797

TABLE 16

$\kappa(M^{-1}A)$ results for MILU ($c_d = 2\pi^2$) preconditioned system for Data Set 2

h_d	MILU	Periodic
1/8	2.629	3.075
1/16	4.393	5.572
1/32	7.987	10.654

TABLE 17

$\kappa(M^{-1}A)$ results for MILU ($c_d = 2\pi^2$) preconditioned system for Data Set 3

h_d	MILU	Periodic
1/8	2.782	2.801
1/16	2.920	2.954
1/32	6.322	6.597

We also analyze the MILU preconditioned operators for the anisotropic data sets. Tables 15, 16, and 17 list the condition numbers for each of the three data sets using the MILU preconditioner with $c_d = 2\pi^2$. Each table includes both the Dirichlet MILU and the calculated Fourier condition number for various values of h_d. Again, the similarity in the dependence of $\kappa(M^{-1}A)$ is noticeable. For all three data sets and for both the Dirichlet and Fourier results $\kappa(M^{-1}A)$ demonstrates $O(h^{-1})$ behavior.

In figures 5 and 6 we have plotted $\kappa(M^{-1}A)$ as a function of c for MILU for the anisotropic data sets 2 and 3, respectively. The upper two curves of each figure correspond to $h_d = 1/32$ and the lower two curves to $h_d = 1/16$. Again, as in the isotropic MILU results, except when c is near zero, the Fourier curves mimic the dependence on c demonstrated by the Dirichlet MILU preconditioned system.

From figures 5 and 6, we can see a difficulty in determining c_{opt} in anisotropic situations. The Dirichlet curves for $\kappa(M^{-1}A)$ are visually flat near the optimal value of c_d. This flatness may indicate that finding c_{opt} is a poorly conditioned numerical task. However, the optimal value for c in the Fourier curves certainly corresponds to a good initial approximation of c_{opt} in the Dirichlet case. By this we mean that by choosing c_d to be the value corresponding to the optimal c determined from the Fourier values that the behavior of $\kappa(M^{-1}A)$ in the Dirichlet problem will be $O(h^{-1})$ rather than $O(h^{-2})$.

5. Conclusions. We note that the Fourier technique used here and in [7] is not exact, but it has been shown to be a powerful tool in the analysis of preconditioned systems. Although the Fourier and Dirichlet condition numbers are not identical, the Fourier method is still capable of predicting the dependence of the Dirichlet condition number on the parameters h and c. In the case of an MILU preconditioner, the Fourier method provides a simple and fast technique to find a first approximation to the optimal c parameter. This makes the method very worthwhile since there are currently no other 'easy' methods to apply that give better results. And this is further emphasized by its easy application to anisotropic problems.

Acknowledgment. The first author would like to acknowledge the helpful discussions with Rosa Donat on the use of Maple in the proof of Theorem 3.2 and to Richard E. Little for general encouragement. Also, many thanks to the reviewers of this paper. Their comments, large and small, were greatly appreciated.

Appendix. In this section, we provide the details of proofs and derivations omitted from the main text: we prove Theorems 3.1 and 3.2 and derive Result 3.1.

THEOREM 3.1. For the ILU preconditioned isotropic operator $(w = 0, c = 0)$,

$$\kappa^{(I)} = O(h^{-2}).$$

Proof. For the isotropic problem $(a_1 = a_2 = a_3 = 1)$ with ILU preconditioner $(w = 0, c = 0)$ we get the recurrence (7) the expression $6 = \alpha + \frac{3}{\alpha}$ whose solution is $\alpha = 3 + \sqrt{6}$ and we have

$$\begin{aligned} \lambda_{str} &= 4(\sin^2(\frac{\theta_s}{2}) + \sin^2(\frac{\phi_t}{2}) + \sin^2(\frac{\xi_r}{2})) \\ \psi_{str} &= \lambda_{str} + \frac{2}{\alpha}(\cos(\theta_s - \phi_t) + \cos(\xi_r - \theta_s) + \cos(\phi_t - \xi_r)) \end{aligned}$$

It holds immediately that

$$\begin{aligned} \lambda_{min} &\geq \lambda_{l.b.} = 12\sin^2(\pi h) \approx 12(\pi h)^2 + O(h^4) \\ \lambda_{max} &\leq \lambda_{u.b.} = 12 \\ \psi_{max} &\leq \psi_{u.b.} = 12 + \frac{6}{\alpha} \end{aligned}$$

Now, for the lower bound on ψ_{str}. Set $x = \sin\frac{\theta_s}{2}, y = \sin\frac{\phi_t}{2}, z = \sin\frac{\xi_r}{2}$ and use that

$$\begin{aligned} \cos(\theta_s - \phi_t) &= 1 - 2(x^2 + y^2) + 4x^2y^2 \pm 4xy\sqrt{(1 - x^2)(1 - y^2)} \\ &> 1 - 2(x^2 + y^2) - 4|xy| \end{aligned}$$

$$\begin{aligned} \psi_{str} &= \lambda_{str} + \frac{2}{\alpha}(\cos(\theta_s - \phi_t) + \cos(\phi_t - \xi_r) + \cos(\xi_r - \theta_s)) \\ &\geq \lambda_{str} + \frac{2}{\alpha}(3 - 2(x^2 + y^2) - 4|xy| - 2(y^2 + z^2) - 4|yz| - 2(x^2 + z^2) - 4|xz|) \\ &= 4(x^2 + y^2 + z^2) + \frac{2}{\alpha}(3 - 4(x^2 + y^2 + z^2) - 4(|xy| + |yz| + |xy|)) \\ &= \frac{4}{\alpha}((\alpha - 2)(x^2 + y^2 + z^2) - 2(|xy| + |yz| + |xy|)) + \frac{6}{\alpha} \\ &= \frac{4}{\alpha}((1 + \sqrt{6})(x^2 + y^2 + z^2) - 2(|xy| + |yz| + |xy|)) + \frac{6}{\alpha} \\ &> \frac{4}{\alpha}(2(x^2 + y^2 + z^2) - 2(|xy| + |yz| + |xy|)) + \frac{6}{\alpha} \\ &= \frac{4}{\alpha}((|x| - |y|)^2 + (|y| - |z|)^2 + (|x| - |z|)^2) + \frac{6}{\alpha} \\ &\geq \frac{6}{\alpha} \end{aligned}$$

In other words,

$$\psi_{min} \geq \psi_{l.b.} = \frac{6}{\alpha}.$$

So, we can now finally we get bounds on the condition number via

$$\begin{aligned}
\mu_{min}^{(I)} &\geq \frac{\lambda_{min}}{\psi_{max}} \geq \frac{12\sin^2(\pi h)}{12+\frac{6}{\alpha}} = \frac{2\sin^2(\pi h)}{2+\frac{1}{\alpha}} \\
\mu_{max}^{(I)} &\leq \frac{\lambda_{max}}{\psi_{min}} \leq \frac{12}{\frac{6}{\alpha}} = 2\alpha \\
\kappa^{(I)} &= \frac{\mu_{max}^{(I)}}{\mu_{min}^{(I)}} \leq \frac{2\alpha}{\frac{2\sin^2(\pi h)}{2+\frac{1}{\alpha}}} \\
&= \frac{\alpha(2+\frac{1}{\alpha})}{\sin^2(\pi h)} \approx \frac{\alpha(2+\frac{1}{\alpha})}{(\pi h)^2} \approx 1.2h^{-2}
\end{aligned}$$

Now we will see that this $O(h^{-2})$ bound is tight.

Let $\theta_s = \phi_t = \xi_r = \pi$, $(r = s = t = (n+1)/2)$, to get $\lambda = 12, \psi = 12 + \frac{6}{\alpha}$. From these we have

$$\mu^{(1)} = \frac{\lambda}{\psi} = \frac{12}{12+\frac{6}{\alpha}} \approx 0.916 = O(1).$$

On the other end, letting $\theta_s = \phi_t = \xi_r = \theta_1 = 2\pi h$, we get for small enough h

$$\begin{aligned}
\lambda &= 12\sin^2(\pi h) \\
\psi &= 12\sin^2(\pi h) + \frac{6}{\alpha} \\
\mu^{(2)} &= \frac{\lambda}{\psi} = \frac{2\sin^2(\pi h)}{2\sin^2(\pi h)+\frac{1}{\alpha}} \approx \frac{2(\pi h)^2 + O(h^4)}{\frac{1}{\alpha} + 2(\pi h)^2 + O(h^4)} \\
&\approx 2\alpha(\pi h)^2 + O(h^4)
\end{aligned}$$

Finally, combining the above, we get

$$\begin{aligned}
\frac{\mu^{(1)}}{\mu^{(2)}} &\approx \frac{1}{(2\alpha+1)\pi^2 h^2 + O(h^4)} \\
&= O(h^{-2})
\end{aligned}$$

And so we have that the bound of $O(h^{-2})$ on $\kappa^{(I)}$ is tight. □

THEOREM 3.2. For the MILU preconditioned isotropic operator ($w = 1$),

$$\kappa^{(M)} = \begin{cases} O(h^{-1}), & \text{if } c > 0; \\ O(h^{-2}), & c = 0. \end{cases}$$

Proof. For the isotropic problem ($a_1 = a_2 = a_3 = 1$) with MILU preconditioner ($w = 1, c \neq 0$) we get for the recurrence (7) the expression $6 + ch^2 = \alpha + \frac{9}{\alpha}$ whose solution is

$$\alpha = 3 + \frac{ch^2}{2} + h\sqrt{3c}\sqrt{1 + \frac{ch^2}{12}}.$$

So we have

$$\begin{aligned}
\lambda_{str} &= 4(\sin^2(\frac{\theta_s}{2}) + \sin^2(\frac{\phi_t}{2}) + \sin^2(\frac{\xi_r}{2})) \\
\psi_{str} &= \lambda_{str} + \frac{2}{\alpha}(\cos(\theta_s - \phi_t) + \cos(\xi_r - \theta_s) + \cos(\phi_t - \xi_r)) - \frac{6}{\alpha} + ch^2 \\
&= \lambda_{str} - \frac{2}{\alpha}(3 - \cos(\theta_s - \phi_t) - \cos(\xi_r - \theta_s) - \cos(\phi_t - \xi_r)) + ch^2
\end{aligned}$$

We first derive a lower bound on $\mu^{(M)}$. Observe that $\psi_{str} \leq \lambda_{str} + ch^2$. Also, for h small enough, there exists $\tilde{c}$ such that $\sin(\pi h) \geq \tilde{c}h$ which yields $\lambda_{str} \geq 12(\tilde{c}h)^2$. Thus, we get the lower bound

$$\begin{aligned}
\mu_{str}^{(M)} &\geq \frac{\lambda_{str}}{\lambda_{str} + ch^2} = \frac{1}{1 + \frac{ch^2}{\lambda_{str}}} \\
&\geq \frac{1}{1 + \frac{c}{12\tilde{c}^2}} \equiv \mu_{l.b.}
\end{aligned}$$

Next we derive the upper bound on $\mu^{(M)}$. We use that $\lambda_{str} \leq 12$. With the aid of the symbolic manipulator Maple [9] we get

$$\frac{3 - \cos(\theta_s - \phi_t) - \cos(\xi_r - \theta_s) - \cos(\phi_t - \xi_r)}{\sin^2(\frac{\theta_s}{2}) + \sin^2(\frac{\phi_t}{2}) + \sin^2(\frac{\xi_r}{2})} \leq 6.$$

Hence,

$$\begin{aligned}
\mu_{str} &= \frac{\lambda_{str}}{\lambda_{str} - \frac{2}{\alpha}(3 - \cos(\theta_s - \phi_t) - \cos(\xi_r - \theta_s) - \cos(\phi_t - \xi_r)) + ch^2} \\
&= \frac{1}{1 - (\frac{2}{\alpha})\frac{3 - \cos(\theta_s - \phi_t) - \cos(\xi_r - \theta_s) - \cos(\phi_t - \xi_r)}{4(\sin^2(\frac{\theta_s}{2}) + \sin^2(\frac{\phi_t}{2}) + \sin^2(\frac{\xi_r}{2}))} + \frac{ch^2}{\lambda_{str}}} \\
&= \frac{1}{1 - (\frac{1}{2\alpha})\frac{3 - \cos(\theta_s - \phi_t) - \cos(\xi_r - \theta_s) - \cos(\phi_t - \xi_r)}{\sin^2(\frac{\theta_s}{2}) + \sin^2(\frac{\phi_t}{2}) + \sin^2(\frac{\xi_r}{2})} + \frac{ch^2}{\lambda_{str}}} \\
&\leq \frac{1}{1 - \frac{1}{2\alpha}(6) + \frac{ch^2}{12}}
\end{aligned}$$

Now we use the approximation $\alpha \approx 3(1 + \frac{1}{3}h\sqrt{3c} + O(ch^2))$ to get for small enough h that $\frac{1}{\alpha} \approx \frac{1}{3}(1 - \frac{1}{3}h\sqrt{3c} + O(ch^2))$ which yields

$$\mu_{str} \leq \frac{1}{\frac{1}{3}h\sqrt{3c} + O(h^2)} \equiv \mu_{u.b.}.$$

So, finally

$$\begin{aligned} \kappa^{(M)} &= \frac{\max \mu_{str}}{\min \mu_{str}} \leq \frac{\mu_{u.b.}}{\mu_{l.b.}} = \frac{1 + \frac{c}{12\bar{c}^2}}{\frac{1}{3}h\sqrt{3c} + O(h^2)} \\ &= \begin{cases} O(h^{-1}), & \text{if } c \neq 0; \\ O(h^{-2}), & c = 0. \end{cases} \end{aligned}$$

Next it is shown that the above bounds are tight.
First consider $\theta_s = \phi_t = \xi_r = \theta_1 = 2\pi h$.

$$\begin{aligned} \lambda_{111} &= 12\sin^2(\pi h) \\ \psi_{111} &= 12\sin^2(\pi h) + \frac{2}{\alpha}(3) - \frac{6}{\alpha} + ch^2 = 12\sin^2(\pi h) + ch^2 \\ \mu_{111}^{(M)} &= \frac{\lambda_{111}}{\psi_{111}} = \frac{12\sin^2(\pi h)}{12\sin^2(\pi h) + ch^2} = \frac{1}{1 + \frac{ch^2}{12\sin^2(\pi h)}} \approx \frac{1}{1 + \frac{ch^2}{12(\pi h)^2}} \\ &= \frac{1}{1 + \frac{c}{12\pi^2}} = O(1). \end{aligned}$$

Now consider $\theta_s = \xi_r = \theta$, and $\phi_t = 2\pi - 2\theta$. Then $\sin\frac{\phi_t}{2} = \sin\theta = 2\sin\frac{\theta}{2}\cos\frac{\theta}{2}$. And $\cos(\phi_t - \theta_s) = \cos(\xi_r - \phi_t) = \cos(3\theta_s)$, $\cos(\xi_r - \theta_s) = 1$. In the expression for ψ we will also use the following

$$\cos(3\theta) = 1 - 18\sin^2\frac{\theta}{2} + 48\sin^4\frac{\theta}{2} - 32\sin^6\frac{\theta}{2}.$$

$$\begin{aligned}
\lambda &= 4(2\sin^2(\frac{\theta}{2}) + 4\sin^2(\frac{\theta}{2})\cos^2(\frac{\theta}{2})) = 8\sin^2(\frac{\theta}{2})(1 + 2\cos^2(\frac{\theta}{2})) \\
&= 24\sin^2(\frac{\theta}{2})(1 - \frac{2}{3}\sin^2(\frac{\theta}{2})) \\
\psi &= \lambda - \frac{4}{\alpha}(1 - \cos(3\theta)) + ch^2 \\
&= \lambda - \frac{4}{\alpha}\Big(18\sin^2\frac{\theta}{2} - 48\sin^4\frac{\theta}{2} + 32\sin^6\frac{\theta}{2}\Big) + ch^2 \\
&= 24\sin^2(\frac{\theta}{2})(1 - \frac{2}{3}\sin^2(\frac{\theta}{2})) \\
&\quad - \frac{4}{3}(1 - \frac{1}{3}h\sqrt{3c} + O(ch^2))\Big(18\sin^2\frac{\theta}{2} - 48\sin^4\frac{\theta}{2} + 32\sin^6\frac{\theta}{2}\Big) + ch^2 \\
&\approx 48\sin^4\frac{\theta}{2} + \frac{4}{9}h\sqrt{3c}(18\sin^2\frac{\theta}{2} - 48\sin^4\frac{\theta}{2}) + O(ch^2) \\
\mu^{(M)} &= \frac{\lambda}{\psi} \approx \frac{24\sin^2(\frac{\theta}{2})(1 - \frac{2}{3}\sin^2(\frac{\theta}{2}))}{48\sin^4\frac{\theta}{2} + \frac{4}{9}h\sqrt{3c}(18\sin^2\frac{\theta}{2} - 48\sin^4\frac{\theta}{2}) + O(ch^2)}
\end{aligned}$$

If $c = 0$, this simplifies to $\mu^{(M)} \approx \frac{1}{2\sin^2(\frac{\theta}{2})}$. Setting $\theta = \theta_1 = 2\pi h$ leads to $\mu^{(M)} = O(h^{-2})$. If $c > 0$, setting $\theta \approx 2\sqrt{h}$ (ie. $s \approx \frac{\sqrt{n+1}}{\pi}$) leads to $\mu^{(M)} = O(h^{-1})$. Hence, we have the exact bounds

$$\kappa^{(M)} = \begin{cases} O(h^{-1}), & \text{if } c > 0; \\ O(h^{-2}), & c = 0. \end{cases}$$

□

Result 3.1. For the MILU preconditioned isotropic operator, the optimal value of c (the one that minimizes $\kappa^{(M)}$) occurs near $c_p = 12\pi^2$ for the periodic problem and $c_d = 3\pi^2$ for the Dirichlet problem.

In the derivation of this result, we make use of the following empirical results: the maximum value of μ occurs on the plane $\theta + \phi + \xi = 2\pi$ (and symmetric planes) where $\theta = \phi$ is small.

So as in the latter part of the proof of Theorem 3.2 we have

$$\mu_{str}^{(M)} \approx \frac{24\sin^2(\frac{\theta}{2})(1-\frac{2}{3}\sin^2(\frac{\theta}{2}))}{48\sin^4\frac{\theta}{2}+\frac{4}{9}h\sqrt{3c}(18\sin^2\frac{\theta}{2}-48\sin^4\frac{\theta}{2})+O(h^2)}$$

Let $x \equiv \sin^2(\frac{\theta_s}{2})$.

$$\begin{aligned}\mu_{str}^{(M)} &\approx \frac{24x(1-\frac{2}{3}x)}{48x^2+\frac{4}{9}h\sqrt{3c}(18x-48x^2)+O(h^2)} \\ &= \frac{24(1-\frac{2}{3}x)}{48x+\frac{4}{9}h\sqrt{3c}(18-48x)+\frac{O(h^2)}{x}} \\ &\approx \frac{24}{48x+\frac{4}{9}h\sqrt{3c}(18-48x)+\frac{O(h^2)}{x}}\end{aligned}$$

In the above and in the rest of the derivation we use that $x << 1$ and hence $x^2 << x$ which can be verified a postiori from the derivation.

Setting $0 = \frac{\partial\mu}{\partial x}$ we get $x^2 \approx \frac{ch^2}{48}$ which implies $\sin^2(\frac{\theta_s}{2}) \approx \sqrt{c/48}h$. Substituting this result back into the equation for $\mu_{max}^{(M)}$ yields

$$\mu_{str}^{(M)} \approx \frac{3}{2\sqrt{3c}h}.$$

For the minimum we use $\theta = \phi = \xi = 2\pi h$ and get

$$\mu_{min}^{(M)} = \frac{12\sin^2(\pi h)}{12\sin^2(\pi h)+ch^2} = \frac{1}{1+\frac{c}{12\pi^2}}.$$

Thus as a function of c,

$$\kappa^{(M)}(c) = \frac{\mu_{max}}{\mu_{min}} = \frac{1+\frac{c}{12\pi^2}}{\frac{2\sqrt{3c}h}{3}}.$$

We want the c value that yields the minimum $\kappa^{(M)}$, hence set $0 = \frac{\partial\kappa}{\partial c}$ to get $c_p \approx 12\pi^2$.

But this is the parameter c for the periodic approximation. To predict the optimal c_d value for the Dirichlet problem we use $\delta_p = c_p{h_p}^2 = \delta_d = c_d{h_d}^2$ as in [7] where $h_p = \frac{h_d}{2}$. And find that

$$c_d \approx \frac{1}{4}c_p = 3\pi^2.$$

REFERENCES

[1] C. Ashcraft and R. Grimes, *On vectorizing incomplete factorizations and SSOR preconditioners,* SIAM J. Sci. Stat. Comp., Vol. 9, No. 1, Jan. 1988, pp. 122-151.

[2] O. Axelsson and V. Eijkhout, *Robust Vectorizable Preconditioners for Three dimensional Elliptic Difference Equations with anisotropy,* 1987.

[3] O. Axelsson and G. Lindskog, *On the eigenvalue distribution of a class of preconditioning methods,* Numer. Math. 48 (1986a), pp. 479-498.

[4] O. Axelsson and G. Lindskog, *On the rate of convergence of the preconditioned conjugate gradient methods,* Numer. Math. 48 (1986b), pp. 499-523.

[5] A. Brandt, *Rigorous Local Mode Analysis of Multigrid,* Weizmann Inst. of Sci., Dept. of Applied Math. & Comp. Sci., Dec. 1988.

[6] T.F. Chan, *Fourier Analysis of Relaxed Incomplete Factorization Preconditioners,* UCLA CAM Report 88-34, Nov. 1988.

[7] T.F. Chan and H.C. Elman, *Fourier Analysis of Iterative Methods for Elliptic Problems,* SIAM Review, Vol. 31, No. 1, March 1989, pp. 20-49.

[8] T.F. Chan and G. Meurant, *Fourier Analysis of Block Preconditioners,* UCLA CAM Report 90-04, Feb. 1990.

[9] B.W. Char, G.J. Fee, K.O. Geddes, G.H. Gonnet and M.B. Monagan, *A Tutorial Introduction to Maple,* J. Symbolic Comp. 2 (1986), pp. 179-200.

[10] H.C. Elman, "Relaxed and Stabilized Incomplete Factorizations for Non-Self-Adjoint Linear Systems," Dept. of Comp. Sci., Jan. 1989.

[11] G.H. Golub and C.F. Van Loan, *Matrix Computations,* Johns Hopkins University Press, 1989.

[12] I. Gustafsson, *A Class of First Order Factorization Methods,* BIT 18 (1978), pp. 142-156.

[13] J.A. Meijerink and H.A. van der Vorst, *An iterative solution method for linear systems of which the coefficient matrix is a symmetric M-matrix,* Math. Comp. 31 (1977), pp. 148-162.

[14] H.A. van der Vorst, *High performance preconditioning,* SIAM J. Sci. Stat. Comput., Vol. 10, No. 6, Nov. 1989, pp. 1174-1185.

[15] H.A. van der Vorst, *ICCG and Related Methods for 3D Problems on Vector Computers,* Comp. Phys. Comm. 53 (1989) 223-235.

[16] G. Wittum, *On the Robustness of ILU Smoothing,* SIAM J. Sci. Stat. Comput., Vol. 10, No. 4, July 1989, pp. 699-171.